LA-UR -80-329

CONF-800809--3

TITLE: ON THE NATURE OF THE BUILDUP TO DETONATION IN SOLID HIGH EXPLOSIVES DURING PLANE SHOCK INITIATION

AUTHOR(S): Jerry J(oel) Dick

MASTER

MASTER

SUBMITTED TO: 18th International Symposium on Combustion

University of California

LOS ALAMOS SCIENTIFIC LABORATORY
Post Office Box 1663 Los Alamos, New Mexico 87545
An Affirmative Action/Equal Opportunity Employer

Form No. 836 R3
St. No. 2629
12/78

UNITED STATES
DEPARTMENT OF ENERGY
CONTRACT W-7405-ENG-36

On the Nature of the Buildup to Detonation in Solid High Explosives during Plane Shock Initiation

J. J. Dick

University of California
Los Alamos Scientific Laboratory
P. O. Box 1663
Los Alamos, New Mexico 87545
USA

(23) Theory of Deflagration and Detonation
(33) Condensed Phase Detonation Initiation

ABSTRACT

Two models for the initiation process are compared to results of experimental studies of initiation of detonation in two high explosives, PBX-9404 (HMX-based) and PBX-9502 (TATB-based), by sustained shock waves. A critical examination of the model known as single-curve buildup is made. Several comparisons are made with experimental results for the two explosives. The model describes the observed shock trajectories moderately well although it has some limitations. These are manifested by an examination of the relation between input pressure and distance of run to detonation. The data are also compared with model solutions for the initiation process which assume self-similar flow. The model can fit the experimental shock trajectory reasonably well but difficulties are encountered in attempting to complete the solution for the entire flow field. For PBX-9404, published pressure-time profiles are examined for self-similar character. The measured profiles show substantial disagreement with the similarity model.

Introduction

Plane shock-initiation of detonation in condensed high explosives has been studied for a number of years. Many experiments have been done with wedge-shaped samples using streak camera recording to obtain the position-time trajectory of the buildup to detonation.[1,2] It has been observed that the trajectories obtained for different input shock pressures have common features. In particular, if the trajectories are plotted together using the transition point as origin, then the trajectories nearly coincide. This has led to the hypothesis concerning the buildup to detonation known as common- or single-curve buildup.[3] This assumption is used in the derivation of the Forest Fire chemical heat release rate function from wedge data.[4,5] In this paper we scrutinize this single-curve assumption and test its validity for the heterogeneous high explosives PBX-9404 (94/3/3 wt%, HMX/nitrocellulose/tris (β-chloro-ethyl)-phosphate) and PBX-9502 (95/5 wt%, TATB/Kel-F 800).

There has also been considerable interest in modeling buildup by self-similar flows. Logan and Perez[6] have derived a class of self-similar solutions for plane shock-initiation of detonation. The solutions restrict the allowed forms of the rate law. It would be possible to specify the rate function parameters from a shock trajectory obtained from a wedge experiment along with a pressure-time record from a manganin gauge at some station such as the input face of the explosive. The solutions give a fairly good fit to the shock trajectory, but some difficulty was met in attempting to obtain solutions for the entire flow field in accord with experimental results. In addition, a set of manganin gauge records in PBX-9404 was examined to test for self-similar flow. The records show substantial disagreement with the self-similar assumption.

Single-Curve Buildup

In a wedge test one obtains the position-time trajectory of the sustained shock wave as it builds up to detonation. Figure 1 shows a schematic diagram of the experiment. Figure 2 shows a digitized position-time trajectory. By using a running linear least squares fit to five data points at a time, one obtains the shock velocity vs distance trajectory as shown in Fig. 3.

The single-curve buildup model assumes, in a coordinate system with its origin at the detonation transition point, that in the buildup to detonation the wave fronts in experiments with different input pressures, P_o, all follow a common trajectory. That is, at a given distance from detonation, the subsequent trajectory is independent of the previous history. The position coordinate is $X = x^* - x_s$, where x^* and x_s are transition point and shock position, respectively, in the coordinate system measuring run-distance from the driver and wedge interface. The common trajectory implies that the local wave velocity, $\frac{dX}{dt}$, is also common; in turn, the curve of wave-front pressure vs distance or time must also be common. Finally, this implies that the sensitivity plot of run-distance vs input pressure is a plot of the common-curve, provided that P_o is replaced by P_s and x^* is replaced by X. P_o is input pressure in the experiment, P_s is shock pressure on the trajectory, x^* is the experimental distance of run to detonation, and X is the distance back from detonation on the common trajectory. I. E. Lindstrom found the model did describe his results for five densities of tetryl.[3] In this paper we will examine this model with respect to data on plastic-bonded explosives PBX-9404 and PBX-9502.

The shock-initiation sensitivity of explosives is often displayed as input shock pressure vs run-distance. It is found empirically that, within experimental error, often the data can be fit by a power law

$$x^* = aP_o^b \quad ; \tag{1}$$

that is, the data lie about a straight line in the log P_o vs log x^* plane (Pop plot).[7] In this case the common-curve trajectory is specified by

$$X = aP_s^b \quad . \tag{2}$$

If the Hugoniot data are fit by a linear shock velocity vs particle velocity relation, $U = c + su$, then the Rankine-Hugoniot jump condition for conservation of momentum yields a relation for the common curve of shock velocity vs common-curve distance

$$U = \frac{c}{2}\left[1 + \left(1 + \frac{4s}{\rho_o c^2}\left(\frac{X}{a}\right)^{1/b}\right)^{1/2}\right] \quad . \tag{3}$$

The P_o vs x^* initiation data is used in obtaining the chemical heat release rate known as Forest Fire. Both single-curve buildup and a power-law fit to the P_o vs x^* data are usually assumed.

The rate law is derived from this in the following way: the differential equations governing conservation of mass, momertum, and energy can be combined with an assumed equation of state relating internal energy, E; pressure, P; volume, V; and reacted mass fraction, λ, to derive the shock-evolution equation[8]

$$\frac{dP}{dt}\Big|_s + \rho_o U \frac{du}{dt}\Big|_s - \rho\left[(u - U)^2 - \bar{c}^2\right]\frac{\partial u}{\partial x} = -\frac{E_\lambda}{E_p} R \quad . \tag{4}$$

The derivatives are evaluated at the shock front; $\bar{c}^2$ is bulk sound speed for the frozen mixture, and R is the Lagrangian reaction rate,

$$R = \frac{\partial \lambda}{\partial t} + u\frac{\partial \lambda}{\partial x} \quad .$$

R can now be determined. E_λ, E_ρ, and $\bar{c}^2$ can be evaluated from the equation of state (Forest Fire uses the HOM equation of state). Unless known from experiments, the particle velocity gradient behind the shock is often set to zero. The time derivatives of P and u can be evaluated using the common-curve and shock Hugoniot obtained from wedge experiments.

This evaluation gives the reaction rate at the shock, $R(P_s, \lambda = 0)$. In the case of Forest Fire, the logarithm of the rate is fit to a polynomial in shock pressure. Then the rate everywhere in the flow is sometimes computed from

$$R(P) = (1 - \lambda)R(P_s = P, \lambda = 0) \quad . \tag{5}$$

In other cases, a reactive Hugoniot is used and some extent of reaction is allowed to take place in the shock front.

Previous work on explosives has shown the common-curve to be valid within the accuracy of the experimental data.[3] However, there are objections to its strict validity. The shock-change equation implies that the growth rate of the shock pressure depends on the particle velocity gradient behind the shock front (Eq. 4). Consider the cases shown in Fig. 4. If an experiment is started at x_1 and P_1, then the pressure and particle velocity gradients will be nearly zero (at the driver and sample interface). If the experiment started out at a much larger distance from detonation transition, then the gradients will probably have developed nonzero values (Fig. 4). In-material gauge measurement results and requirements for shock growth suggest this. In fact, the sets of U vs x curves measured in wedge experiments are consistent with this suggested discrepancy (Fig. 5).

Experimentally determined wedge trajectories for PBX-9404 and PBX-9502 are shown in Fig. 5.[9] They are plotted in the common-curve coordinate system so that only the part of the trajectory up to detonation transition is shown.

Within a certain band they do show commonness in the acceleration to detonation. As noted earlier, for some shorter runs the initial part of the run is not on the common-curve and is consistent with the arguments against commonness based on the shock-evolution equation and the experimental boundary condition.

In Fig. 6, the mean experimental curve is compared to the one predicted from the sensitivity and Hugoniot parameters, as well as to a common-curve fit to the mean experimental curve. PBX-9404 is a more sensitive explosive than PBX-9502. This is illustrated by the fact that PBX-9404 will transit to detonation in a run-distance of 20 mm starting from an initial shock speed which is a much smaller fraction of detonation velocity than is the case for PBX-9502. We see that the fit using Eq. 3 does a reasonable job of fitting the mean experimental trajectory for both explosives. However, the fit to Eq. 3 gives a more gradual acceleration than the mean experimental trajectory shows. Not surprisingly, the trajectory generated by using values of a and b from a fit to Eq. 1 agrees with the experimental curve less well. It is a test of the single-curve buildup model.

The agreement can be checked in another way. Equation 3 can be fit to the experimental U vs x curve and values of the parameters a and b can be determined, given values for c and s. These parameter values can be compared to those obtained from fitting the sensitivity data directly. Table I, Fig. 6 and 7 show the comparison. This comparison is quite sensitive and as shown in Fig. 7, there is some disagreement between the experimental line and the line deduced from a fit to the mean experimental trajectory using Eq. 3. The deviation is about the same for both explosives considered here. In a previous analysis on rocket propellants the agreement was fairly good for an insensitive propellant, but there was serious disagreement for some sensitive propellants.[10]

Similarity Solutions

Similarity solutions as models for the shock-initiation process have received some attention in recent times.[6,11] Logan and Perez determined the class of self-similar solutions to the one-dimensional, time-dependent reactive-flow problem, assuming a γ-law equation of state. The solution puts some restrictions on the form of the rate law. The form is

$$R = \left(\frac{p}{p_o}\right)^{\beta} F\left(V, \frac{\lambda}{p}, \frac{u^2}{p}\right) , \qquad (6)$$

where F is an arbitrary function of the variables. The requirement of frame indifference eliminates the possibility of dependence on u^2. It turns out that the exponent β can be determined from an initiation trajectory. The fitting form is

$$U = c_2 \frac{x^*}{t^*} \left(\frac{X}{x^*}\right)^{\frac{c_2-1}{c_2}} , \qquad (7)$$

where $c_2 = (\beta - \frac{3}{2})/(\beta - 1)$ and t* is the time between shock arrival at the input face of the explosive and detonation transition. Values of the exponent β were four and five for PBX-9404 and PBX-9502, respectively. Similarity solutions allow but do not require single-curve buildup. The fit is compared to an experimental PBX-9404 trajectory in Fig. 8. The fit looks reasonable but it proves difficult to find a form for F in Eq. 6 such that the flow-field solution extends out to any sizeable degree of reaction, before a singularity is reached. The large values of pressure exponent β apparently act to quench the reaction too rapidly when P is less than P_o. In contrast, Ref. 6 used a value of β near 2.

It seemed worthwhile to test the degree to which the initiation process is self-similar. J. Wackerle, et. al.,[12] has published a set of manganin gauge pressure-time profiles for shock-initiation of PBX-9404 with P_o = 2.9 GPa.

These profiles are plotted in terms of self-similar variables in Fig. 9. If the flow were self-similar (within the assumptions made), then the profiles should superimpose in this plot. Since they do not, we have an indication that the shock-initiation process in heterogeneous high explosive may not be self-similar.

Conclusions

A comparison has been made between experimental shock-initiation-of-detonation data for PBX-9404 and PBX-9502 and two models of the process. It was found that there is some disagreement between experimental results and the single-curve buildup model, but perfect agreement is not expected. So there may be some justification for use of the model. For the self-similar flow model there is some difficulty in obtaining solutions which fit the experimental results. And an examination of measured pressure-time histories in PBX-9404 shows some disagreement with the self-similar model.

Acknowledgements

I thank J. B. Bdzil, C. Forest, and J. D. Logan for helpful discussions. The work was supported by the U. S. Department of Energy.

References

1. Campbell, A. W.; Davis, W. C.; Ramsay, J. B.; and Travis, J. R.: Phys. Fluids 4, pp. 511-521 (1961).
2. Jacobs, S. J.; Liddiard, T. P., Jr.; and Drummer, B. E.: Ninth Symposium (International) on Combustion, p. 517, The Combustion Institute, 1963.
3. Lindstrom, I. E.: J. Appl. Phys. 41, pp. 337-350 (1970).
4. Forest, C. A.: "Burning and Detonation." Los Alamos Scientific Laboratory Report LA-7245 (July, 1978).
5. Mader, C. L.: Numerical Modeling of Detonation, p. 208, University of California Press, 1979.
6. Logan, J. D. and Perez, J. J.: to be publishe in SIAM J. Appl. Math.
7. Ramsay, J. B. and Popolato, A.: The Fourth Symposium (International) on Detonation, p. 233, (Office of Naval Research), 1965.
8. Fickett, W. and Davis, W. C.: Detonation, p. 131, (University of California Press), 1979.
9. Craig, B. G. and Ramsay, J. B.: unpublished data.
10. Dick, J. J.: 16th JANNAF Combustion Meeting, Chemical Propulsion Information Agency, 1979, to be published.
11. Cowperthwaite, M.: Symposium H.D.P., p. 201, Commissariat a l'Energie Atomique, 1978.
12. Wackerle, J.; Rabie, R.L.; Ginsberg, M.J.; and Anderson, A. B.: Symposium H.D.P., p. 127, Commissariat a l'Energie Atomique, 1978.

Table I

Comparison of Initiation Parameters; Test of Common Curve Model with Power Law Fit (Eq. 1)

Formulation	Parameters Fit to x^*-P_0 Data (Eq. 1)		Parameters Fit to Mean Trajectory (Eq. 3)	
	a	b	a'	b'
PBX-9404	45	-1.47	29	-1.26
PBX-9502	3 900	-2.40	6 600	-2.71

Figure Captions

Figure 1. Geometry of the wedge test. The last attenuator plate PMMA (Plexiglas) drives a shock wave into the explosive wedge. Interaction of the wave front with the wedge face is recorded on a rotating mirror camera. The needle image reflected from the aluminized PMMA surface provides a record of driver free-surface velocity.

Figure 2. A digitized t vs x trajectory obtained from a streak record.

Figure 3. Shock velocity and wave front pressure vs run-distance derived from the trajectory of Fig. 2.

Figure 4. Shock pressure and pressure gradient vs run-distance. For an experiment beginning at x_1, the pressure gradient will be nearly zero at x_1. For a longer run where the wave has traveled a good distance before reaching x_1, the gradient at x_1 will probably be strongly negative as shown.

Figure 5. Measured shock velocity vs distance curves for PBX-9404 and PBX-9502. The distance axis origin is at the detonation transition.

Figure 6. Common curve shock velocity vs distance trajectories for PBX-9404 and PBX-9502. The mean experimental trajectory is shown along with common-curves calculated from Eq. 3 using parameters a and b obtained from fits to Eqs. 1 and 3, respectively.

Figrue 7. Comparison of the lines generated by fit to P_o vs x* data (Eq. 1) with that obtained by fitting U vs X data (Eq. 3). Comparison is made for PBX-9404 and PBX-9502.

Figure 8. Shock velocity vs distance trajectory for PBX-9404 from a wedge initiation experiment is compared to a fit to the trajectory based on a self-similar flow model. P_o = 2.9 GPa.

Figure 9. A set of pressure-time profiles measured in initiating PBX-9404, P_o = 2.9 GPa, (Ref. 11) are plotted in self-similar coordinates; a dimensionless pressure, $\hat{P} = (P/P_o)(1 - t/t^*)^{2(1-c_2)}$, and the self-similar dimension $s = (1 - x/x^*)/(1 - t/t^*)^{c_2}$ where $c_2 = (\beta - 3/2)/(\beta - 1)$. The profiles should coincide if the flow is in agreement with the self-similar model.

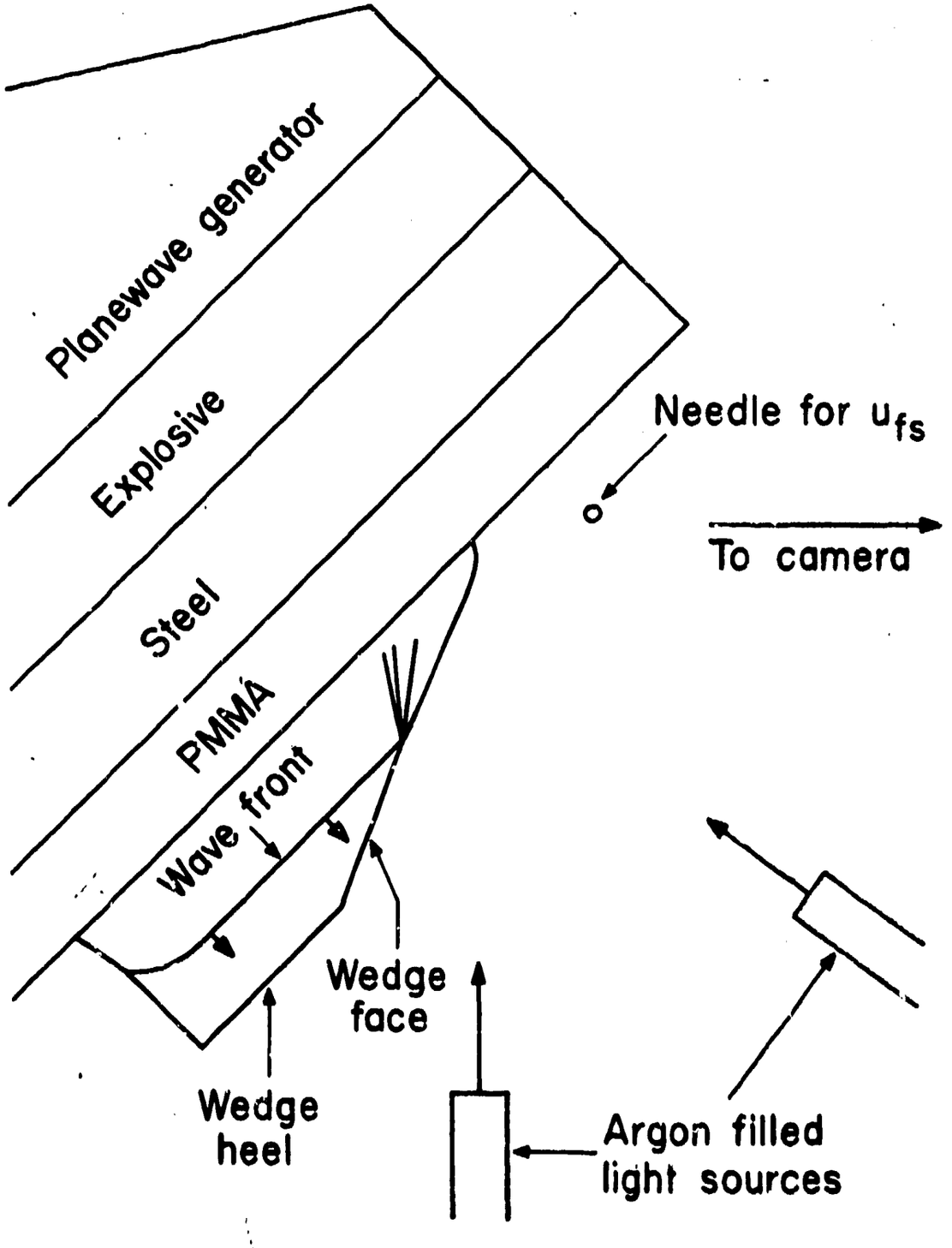
Planewave generator
Explosive
Steel
PMMA
Wave front
Needle for u_{fs}
To camera
Wedge face
Wedge heel
Argon filled light sources

Fig. 1.

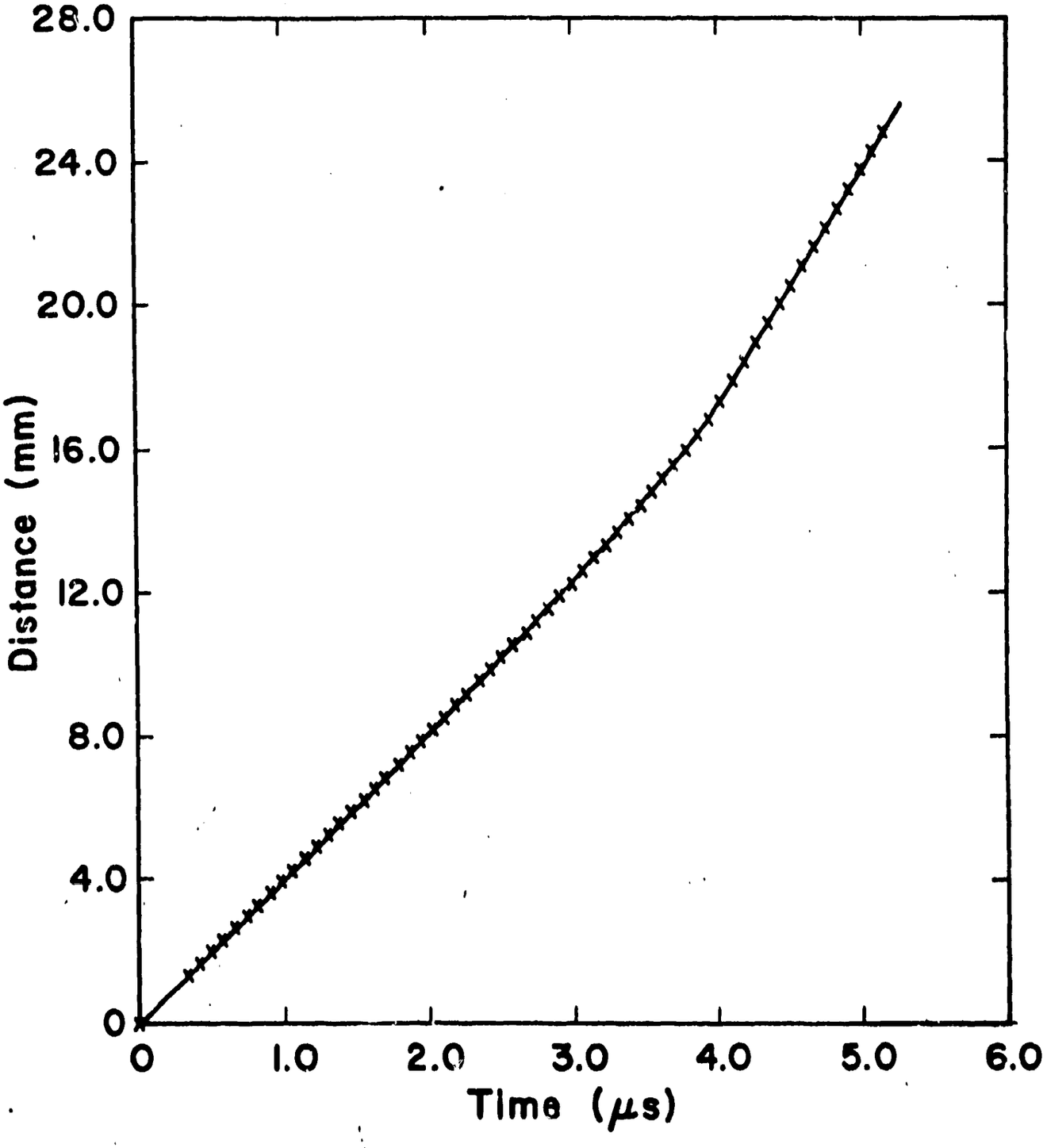

Fig. 2.

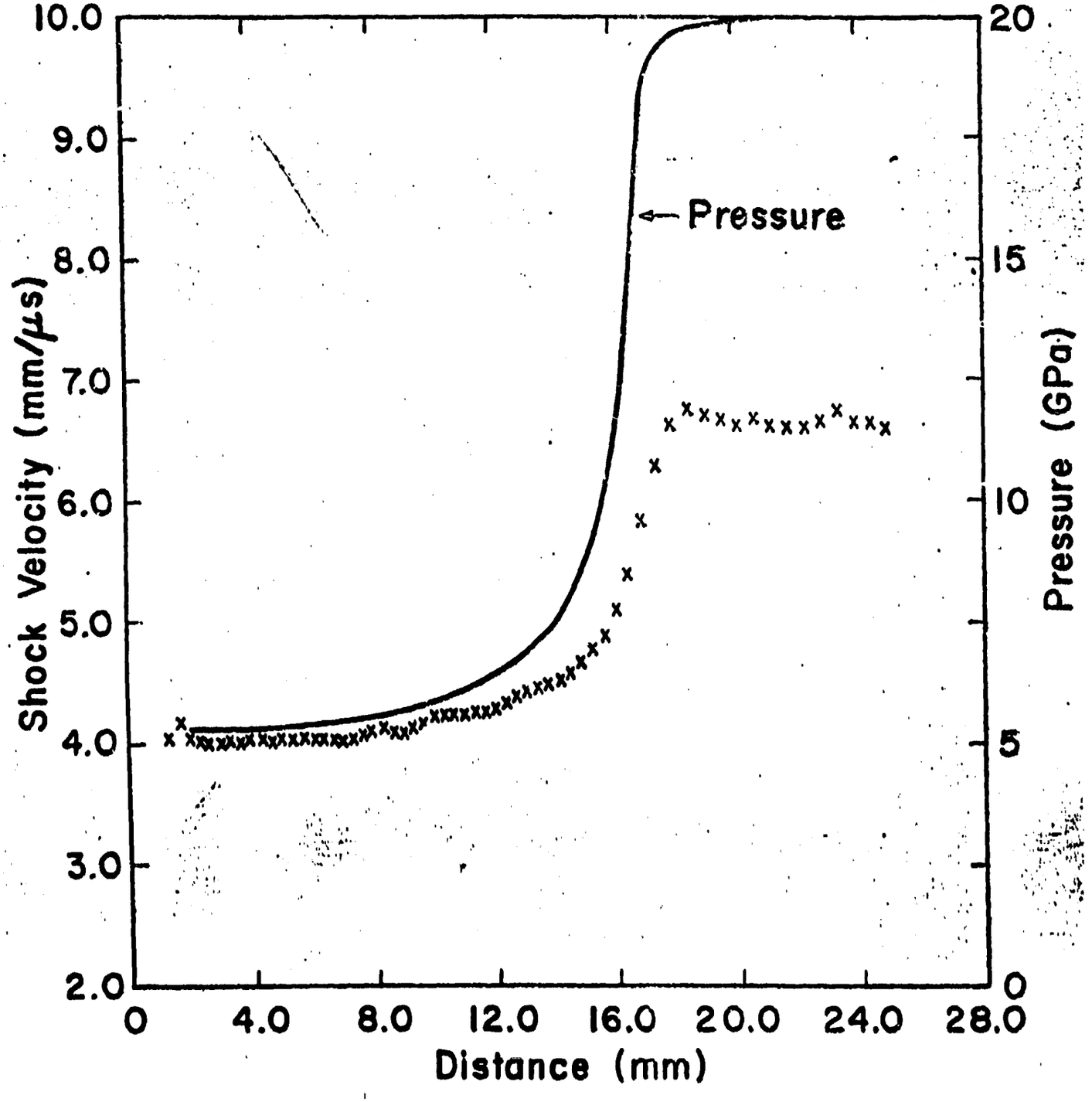
10.0
9.0
8.0
7.0
6.0
5.0
4.0
3.0
2.0
Shock Velocity (mm/μs)
20
15
10
5
0
Pressure (GPa)
← Pressure
0
4.0
8.0
12.0
16.0
20.0
24.0
28.0
Distance (mm)

Fig. 3.

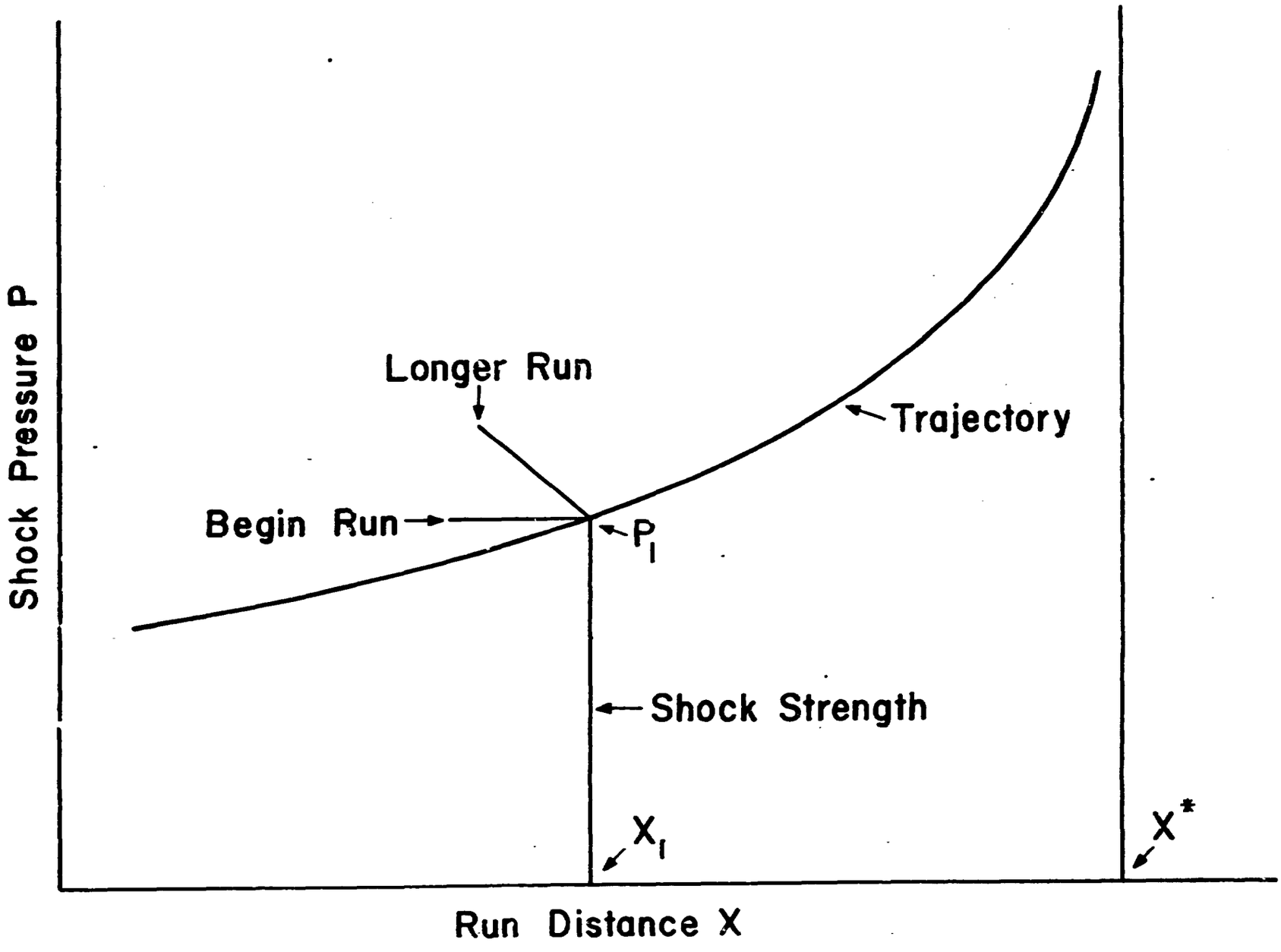
Shock Pressure P
Longer Run
Trajectory
Begin Run
P_1
Shock Strength
X_1
X^*
Run Distance X

Ftg. 4.

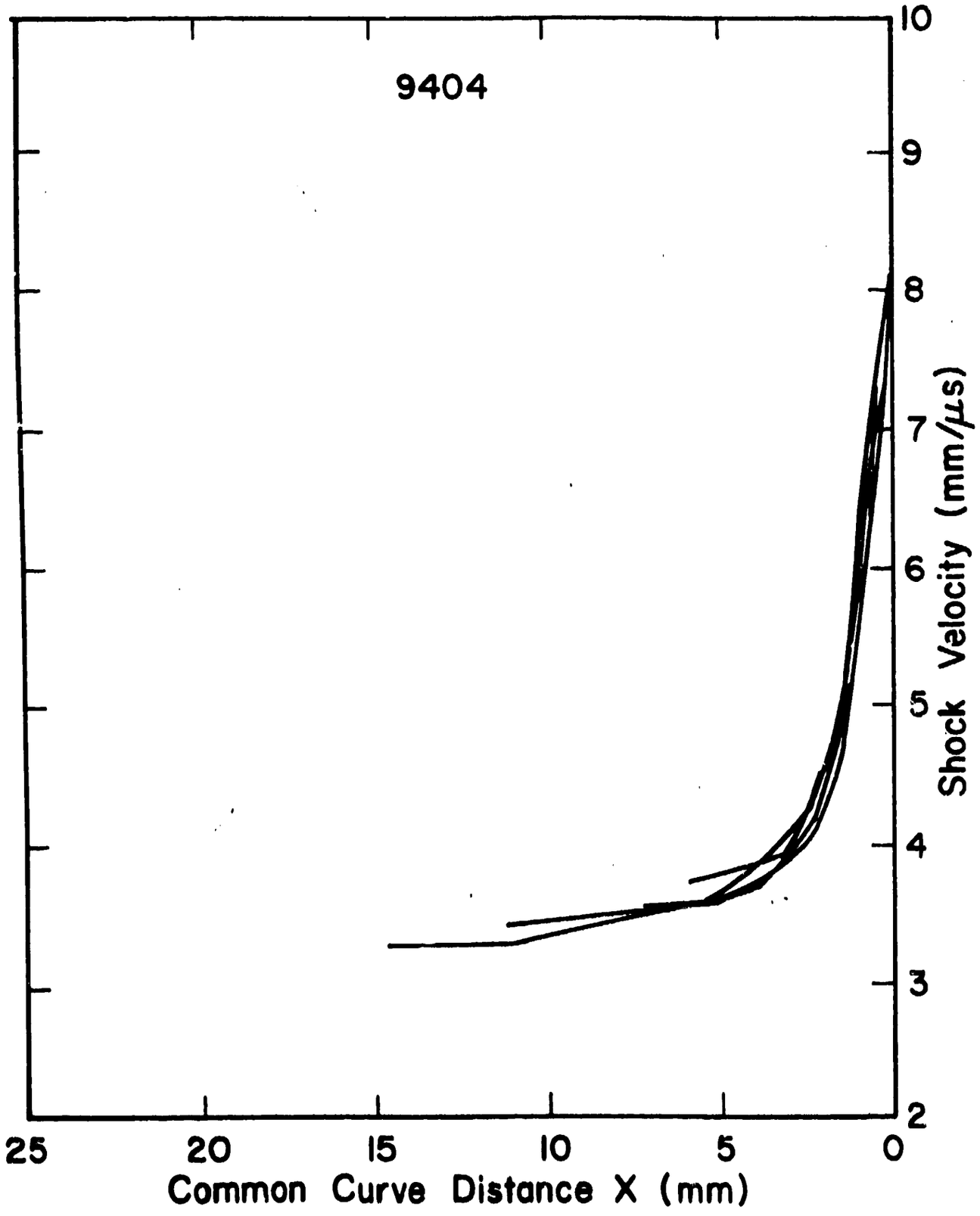
9404
10
9
8
7
6
5
4
3
2
Shock Velocity (mm/μs)
25
20
15
10
5
0
Common Curve Distance X (mm)

Fig. 5a.

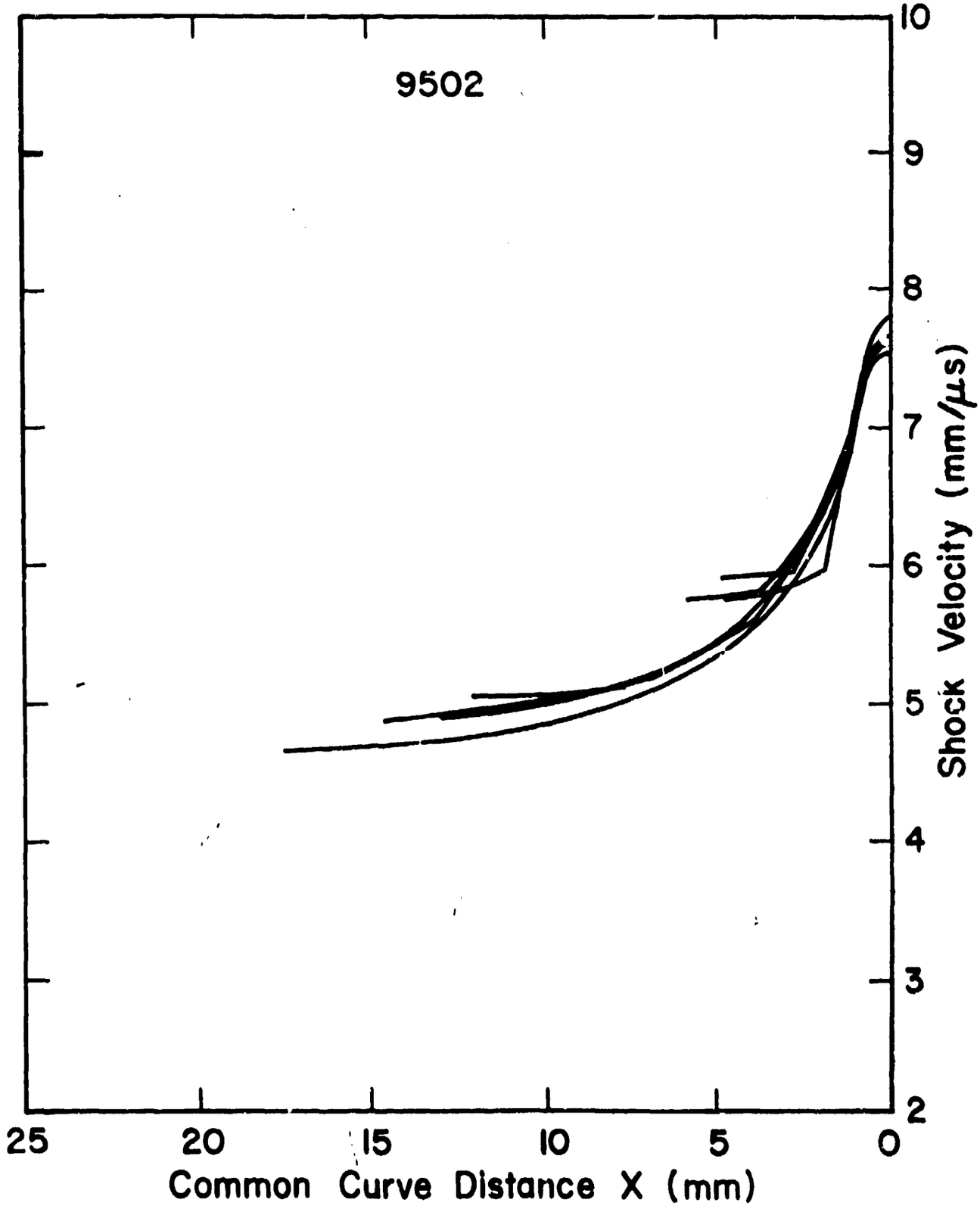
9502
10
9
8
7
6
5
4
3
2
Shock Velocity (mm/μs)
25
20
15
10
5
0
Common Curve Distance X (mm)

Fig. 5b.

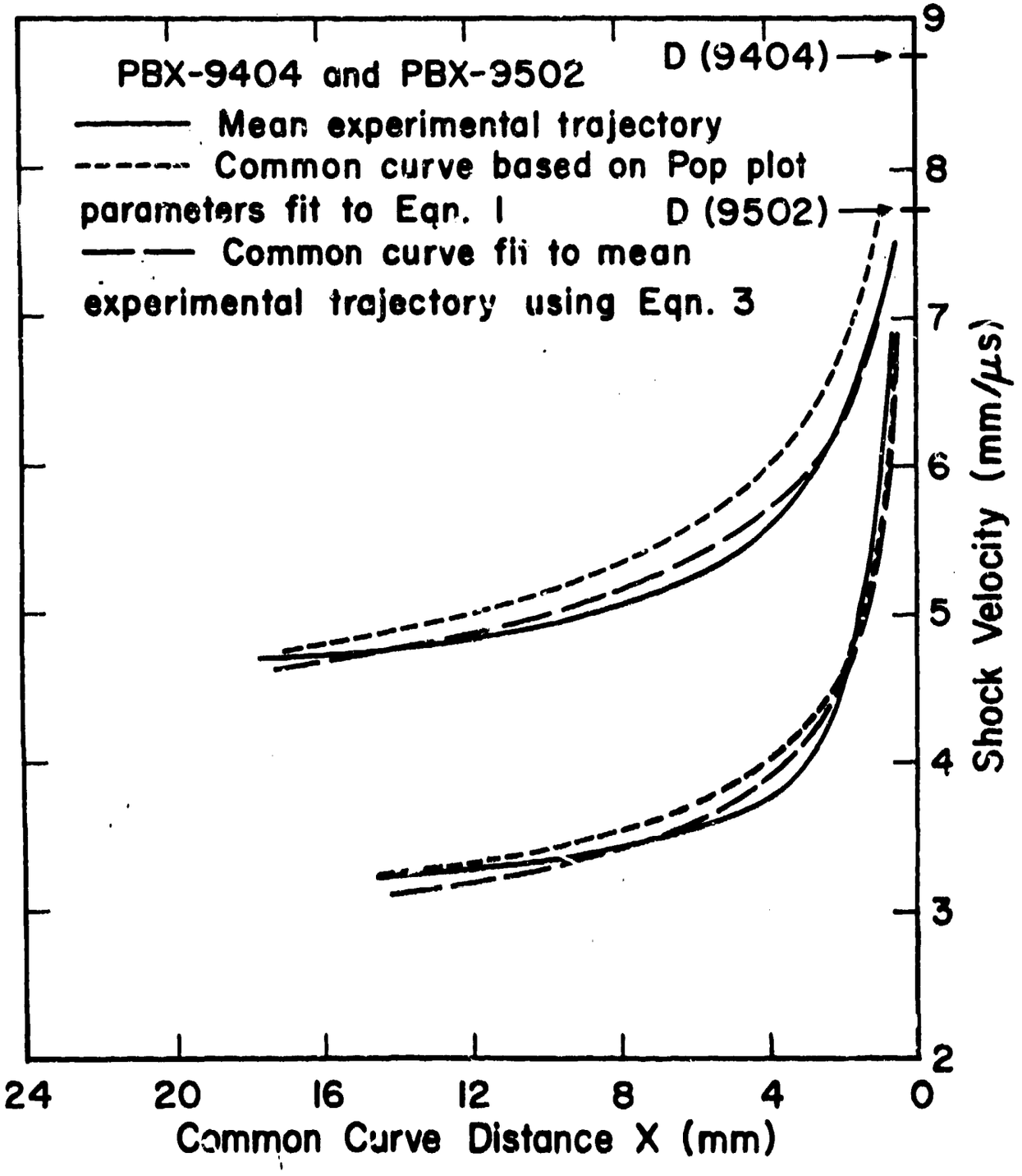
PBX-9404 and PBX-9502
D (9404)
Mean experimental trajectory
Common curve based on Pop plot parameters fit to Eqn. 1
D (9502)
Common curve fit to mean experimental trajectory using Eqn. 3
Shock Velocity (mm/μs)
9
8
7
6
5
4
3
2
24
20
16
12
8
4
0
Common Curve Distance X (mm)

Fig. 6.

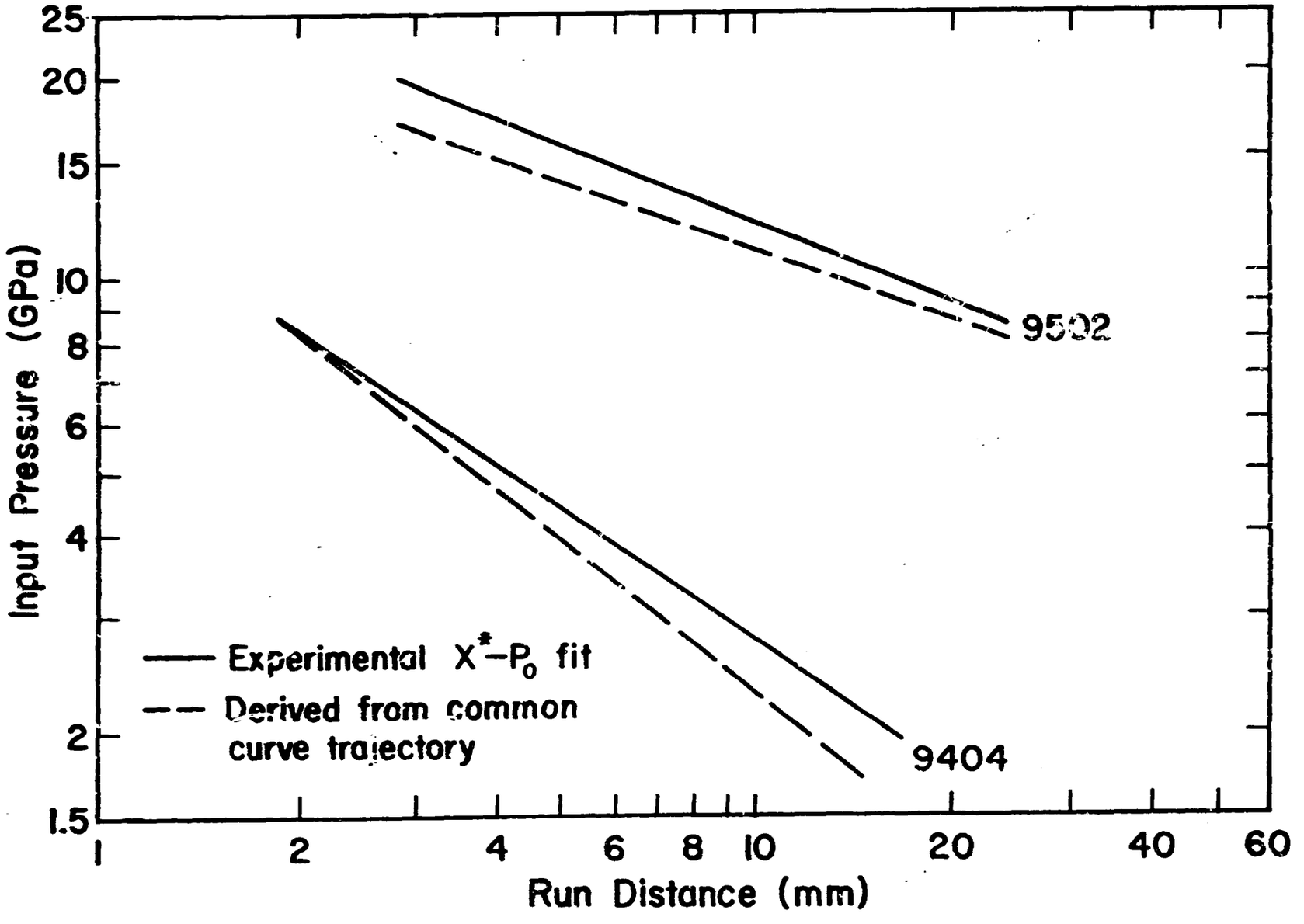
25
20
15
10
8
6
4
2
1.5
Input Pressure (GPa)
9502
9404
Experimental X^*-P_0 fit
Derived from common curve trajectory
1
2
4
6
8
10
20
40
60
Run Distance (mm)

Fig. 7.

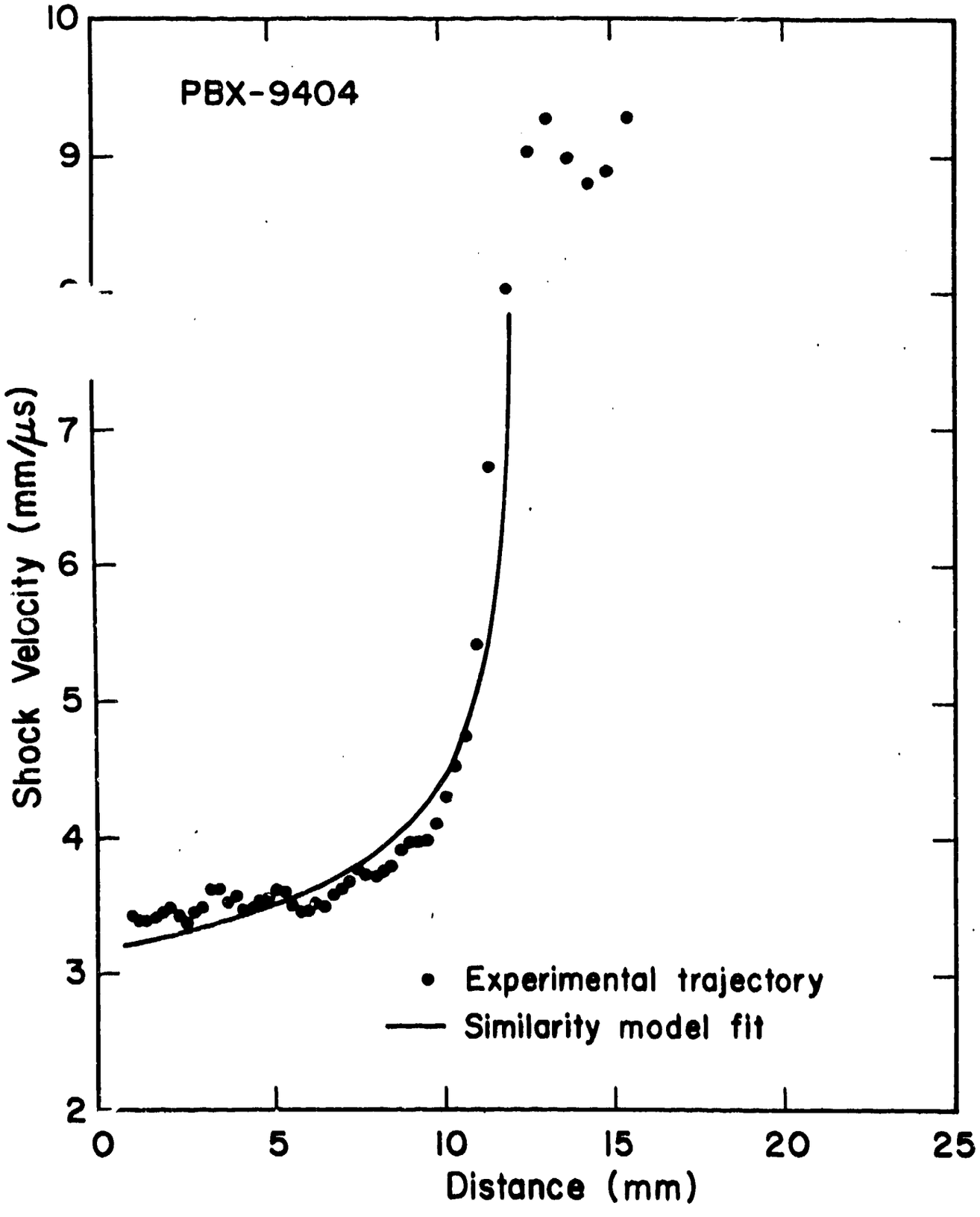
PBX-9404
Shock Velocity (mm/μs)
Distance (mm)
Experimental trajectory
Similarity model fit
10
9
7
6
5
4
3
2
0
5
10
15
20
25

Fig. 8.

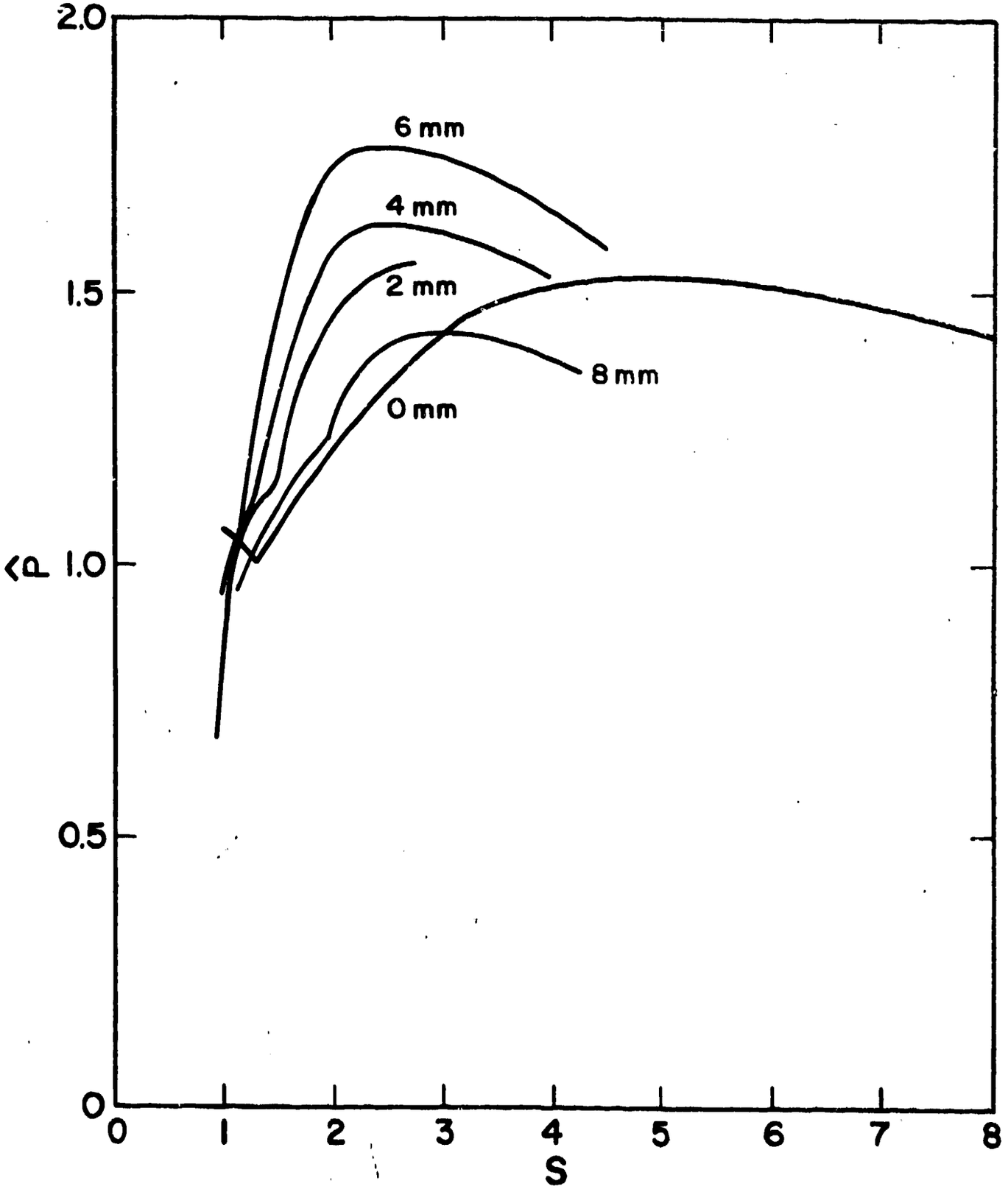

Fig. 9.